A STUDY ON THE RESPONSE OF CES STRUCTURE WITH DIFFERENT SHEAR STRENGTH OF BEAM-COLUMN JOINTS

Kazuki Takahashi[1], Tomofusa Akita[2] and Eiichi Inai[3]

1. Graduate student, Graduate School of Sciences and Technology for Innovation, Yamaguchi Univ.
2. Lecturer, Graduate School of Sciences and Technology for Innovation, Yamaguchi Univ. Dr. Eng.
3. Prof, Graduate School of Sciences and Technology for Innovation, Yamaguchi Univ. Dr. Eng.
Email: i034ve@yamaguchi-u.ac.jp, akita@yamaguchi-u.ac.jp, inai@yamaguchi-u.ac.jp

ABSTRACT

CES (Concrete Encased Steel) structure is a new structure composed of steel and fiber reinforced concrete (FRC). Comparing the SRC structure and the CES structure, the CES structure can shorten the construction period, reduce the construction cost and facilitate the pre-casting. The Architectural Institute of Japan is trying to publish guidelines for structural performance evaluation to disseminate the CES structure. One of the problems is modeling of the beam-column joint. In the guideline, the beam-column joint is assumed to be rigid as a general rule, but the conditions that can be treated as rigid are unknown. In this study, the authors analyzed CES buildings with different shear strength of beam-column joints and clarified the relationship between the shear strength of beam-column joint and the seismic response.

Keywords: CES structure, different shear strength of beam-column joint, panel zone model, rigid zone model, modal adaptive pushover analysis, time history response analysis

INTRODUCTION

CES (Concrete Encased Steel) is a new structure composed of steel and fiber reinforced concrete (FRC), and has recently been developed as a next-generation composite structural system (Kuramoto, 2005). At the same time as development of CES structure, a guidelines of CES structure (Architectural Institute of Japan, 2013) is preparing. In previous studies (Inoue, 2015; Nakano, 2016), CES buildings were evaluated based on the proposed evaluation method, and the applicability of the evaluation method was examined. At the same time, they examined the influence of modeling of beam-column joints on seismic performance. However, the condition that the beam-column joints can be treated as rigid is not clear. Also, the influence of the modeling of the beam-column joints on the response has not been studied. In this study, the authors analyzed CES buildings with different shear strength of beam-column joints and clarified the relationship between the shear strength of beam-column joints and the seismic response. In the static analysis, the authors calculated the response of equivalent single-degree-of-freedom system and clarified the relationship between beam-column joints shear strength and response. In the dynamic analysis, the seismic response was calculated and the relationship between the beam-column joints shear strength and response was examined.

SEISMIC PERFORMANCE EVALUATION METHOD

Structural experiments of CES columns and beams, beam-column joints, seismic walls and frames are being conducted to create the guidelines for evaluating structural performance of CES structure (Matui, 2011; Suzuki, 2011; Shi, 2012). The evaluation method for the beam-column joints in this study is based on the performance evaluation on CES beam-column joints (Architectural Institute of Japan, 2013). Figure 1 shows restoring force characteristics of the beam-column joints. Here, Q_{jc} is shear crack force, Q_{ju} is ultimate shear force, γ_{jc} is shear deformation angle at shear cracking, γ_{ju} is shear deformation angle at ultimate shear force, and GA is initial stiffness. In addition, it is supposed that the beam-column joints are modeled by the trilinear restoring force characteristic which has a shear crack

point and a shear yield point in principle. However, if the beam-column joints can be considered to be rigid, it may be assumed to be a rigid.
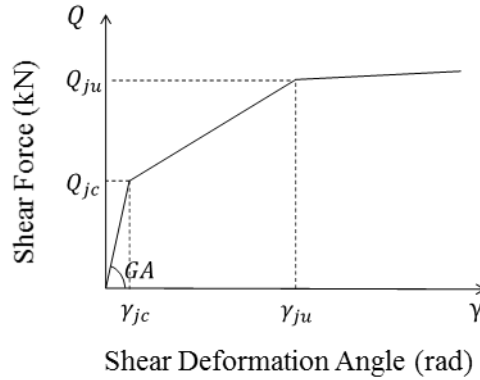
Figure 1. Restoring force characteristics of the joints

ANARYSIS BUILDING

13 story CES office building with the spreading foundation described in previous resarch (Imai, 2015) was analyzed. The building area is 775 m^2, the total floor area is 10,075 m^2, the maximum height is 52.5 m, and the standard floor height is 3.90 m. Figure 2 shows the framing plan and the framing elevation of the building, and Table 1 shows the cross section of each member (column, seismic wall and beam). X direction of the building is 5 spans (span length 6m) in a frame structure, and the Y direction is 3 spans (span length 8m) in a wall frame structure combining multi-story shear walls. The multi-story shear wall is located between Y3 and Y4 on X2 frame and X5 frame. The columns and beams are composed of CES, the wall is composed of reinforced concrete, and the slab is composed of reinforced concrete. The minimum stiffness ratio of each story of the building is 0.742 (5F) in the X direction and 0.766 (8F) in the Y direction. The maximum value of the eccentricity ratio of each story is 0 in both directions, thus the building has no eccentricity. The shear margin ($_cQ_{pu}$ / $_cQ_{bu}$: $_cQ_{pu}$ and $_cQ_{bu}$ are the values obtained by converting the joint panel shear ultimate strength and the beam bending ultimate strength into column shear force) of all joints are over 1.0 and the analysis building is a beam yield type building.
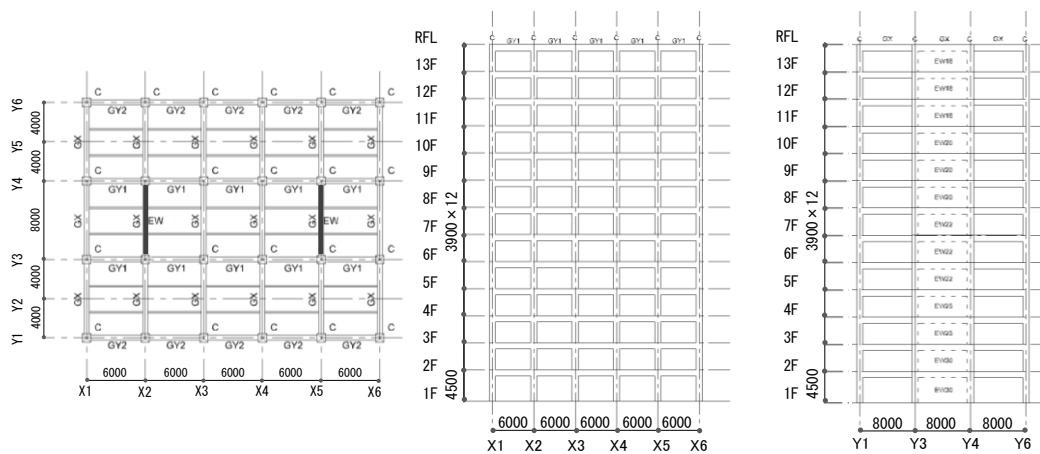
Figure 2. Framing plan and the framing elevation of the building for the analysis

2

Table 1. The cross section of each member (column, seismic wall, beam)

Floor	Column			Seisimic Wall		
	Fc	B×D	Steel Frame Size C	Sign	Wall Thickness	Reinforcement
RF	-	-	-	-	-	-
13F	30	800×800	H-600×300×9×22	EW18	180	D13@200double
12F						
11F						
10F	33	850×850	H-650×350×9×19	EW20	200	D13@150double
9F						
8F						
7F			H-650×350×9×25	EW22	220	D13@100double
6F						
5F						
4F	36	900×900	H-700×400×9×22	EW25	250	D16@150double
3F						
2F			H-700×400×16×25	EW30	300	D19@175double
1F						

Floor	Beam					
	B×D	Steel Frame Size GX	B×D	Steel Frame Size GY1	B×D	Steel Frame Size GY2
RF	500×900	H-700×300×9×16	500×900	H-700×300×9×16	500×900	H-700×300×9×16
13F						
12F				H-700×300×9×19		
11F		H-700×300×9×19				H-700×300×9×19
10F				H-700×300×12×22		
9F		H-700×300×12×19				
8F				H-700×300×12×25		H-700×300×12×22
7F		H-700×300×12×22				
6F						
5F				H-700×300×12×18		H-700×300×12×25
4F						
3F						
2F	500×1000	H-800×300×12×22	500×1000	H-800×300×12×22	500×1000	H-800×300×12×22
1F	-	-	-	-	-	-

ANALYSIS OUTLINE

Modeling and Analysis Method

A three-dimensional frame model is used. The members are replaced with line element and assumed to be a rigid floor. Beams are considered with bending springs and shear springs. Columns and shear walls are modeled by MS (Multi Spring) model in axial direction and bending, and modeling of shear is performed by single axis shear spring. In addition, the resistance hinge length of the MS model is half of the column depth. In order to study the modeling of beam-column joints, the beam-column joints are modeled as rigid zone and panel zone models. The member length of the rigid zone model and the member length of the panel zone model are the same.

Static Analysis

In static analysis, MAP (Modal Adaptive Pushover) analysis proposed in existing resarch (Kuramoto, 2004) is performed. MAP analysis is a method that can use a lateral load pattern which is proportional plastic first mode. The MAP analysis was terminated when the maximum story drift angle reached $R_{max} = 0.02$ rad. At that time, the beam-column joint did not yield.

Dynamic Analysis

In dynamic analysis, the authors used Takeda-Model for beam bending and elastic model for shear. In addition, the damping constant was set to be instantaneous stiffness proportional type, and was 3% with respect to the first natural period. The seismic waves used in this analysis are three waves of EL Centro NS (1940), Hachinohe EW (1968) and Taft EW (1952). Table 2 shows the maximum acceleration, maximum velocity and duration of the three seismic waves used. The strength of three seismic waves was standardized to 50 and 75 cm/s, and the analysis was performed with a total of six types of seismic waves.

Analysis Case

The rigid zone model is called Model-R, and the panel zone model is called Model-PT (corresponding to the minimum share margin value 1.1 of the +-shape in the X direction). Furthermore, in order to investigate the influence of joint shear margin, the minimum value of the shear margin of the +-shape in the X direction of the panel zone model change to 1.0, 1.2, 1.3, 1.4 and 1.5. In controlling the shear margin, the strength and the rigidity of joint was changed uniformly, and they were called Model-m10, Model-m12, Model-m13, Model-m14, and Model-m15, respectively. Table 3 shows the joint shear margin of each model. Table 4 shows the natural period of Model-R and Model-PT. Model-PT is about 8% longer than Model-R in the first natural period in the X direction. Further, Model-PT is about 7% longer than Model-R in both the second natural period and the third natural period in the X direction. No significant difference is found between Model-R and Model-PT in the Y direction.

Table 2. Maximum acceleration, maximum velocity and duration of the three seismic waves

Seismic Wave	Maximum Acceleration (cm/s^2)	Maximum Velocity (cm/s)	Duration (s)
EL Centro NS	341.70	33.59	53.74
Hachinohe NS	229.65	34.56	50.98
Taft EW	175.90	17.49	54.38

Table 3. The joint shear margin of each model

		Model-m10			Model-PT(m11)			Model-m12		
Direction	Shape	Maximum	Minimum	Average	Maximum	Minimum	Average	Maximum	Minimum	Average
X Direction	+-Shape	1.46	**1.02**	1.22	1.49	**1.11**	1.31	1.64	**1.21**	1.42
	T-Shape	2.21	1.43	1.76	2.28	1.60	1.92	2.57	1.81	2.14
Y Direction	+-Shape	1.52	1.10	1.27	1.52	1.19	1.36	1.58	1.31	1.47
	T-Shape	2.30	1.55	1.81	2.30	1.73	1.98	2.37	1.96	2.21
		Model-m13			Model-m14			Model-m15		
Direction	Shape	Maximum	Minimum	Average	Maximum	Minimum	Average	Maximum	Minimum	Average
X Direction	+-Shape	1.79	**1.32**	1.54	1.91	**1.40**	1.63	2.05	**1.51**	1.75
	T-Shape	2.86	2.02	2.39	3.10	2.19	2.57	3.39	2.40	2.81
Y Direction	+-Shape	1.72	1.42	1.60	1.83	1.52	1.69	1.98	1.82	1.63
	T-Shape	2.65	2.19	2.47	2.88	2.38	2.66	3.17	2.91	2.61

Table 4. The natural period of Model-R and Model-PT

	Model-R		Model-PT	
	X Direction	Y Direction	X Direction	Y Direction
Mode	Period (sec)	Period (sec)	Period (sec)	Period (sec)
1st	1.045	0.859	1.129	0.889
2nd	0.354	0.257	0.381	0.263
3rd	0.205	0.132	0.22	0.134

THE RESPONSE OF THE EQUIVALENT SINGLE-DEGREE-OF-FREEDOM SYSTEM

Difference Due to Shear Strength of Beam-Column Joint

Figure 3 shows the relationship between the representative shear strength ($_1Sa$) and the representative displacement ($_1Sd$) of each model. $_1Sa$ and $_1Sd$ were calculated according to the paper (Kuramoto, 2004). The rigidity and the strength of Model-R are larger than that of Model-PT (m11) in both X and Y directions, and the difference is larger in the X direction. The rigidity and the strength of the panel zone models are gradually closing to that of Model-R as the shear margin increases in both X and Y directions.
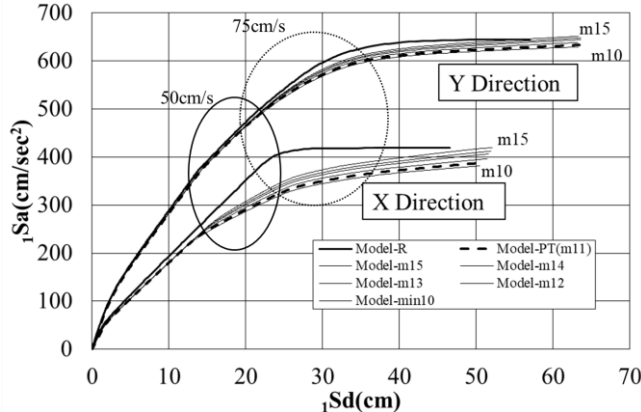
Figure 3. The relationship between the representative shear strength ($_1Sa$) and the representative displacement ($_1Sd$) of each model

Response Spectrum

Figure 4 shows the response of the equivalent single-degree-of-freedom system of Model-R and Model-PT in the X direction according to the response spectrum method described in existing research (Kuramoto, 2001), and Table 5 shows the response of each model and the equivalent period (T_e) at the response. Model-PT (share margin 1.1) has larger representative displacement and equivalent period than Model-R. While Model-PT has smaller representative shear strength than Model-R. In addition, as the joint shear margin increases, the representative displacement decreases and the representative shear strength increases in both the X and Y directions. However, the difference in representative displacement of the panel zone model was quite small. Figure 5 shows the relationship between the response ratio of $_1Sd$ and the joint shear margin. The response ratio of $_1Sd$ is the representative displacement of the panel zone models in the X and Y directions divided by the representative displacement of Model-R. The response ratio was 5 to 6.5% in the X direction and 2 to 3.4% in the Y direction. Therefore, the panel zone model has larger representative displacement than the rigid zone model. The response ratio decreases as the joint shear margin increases in both the X and Y directions. In addition, the increment of representative displacement with increasing shear margin in the Y direction was smaller than that in the X direction due to the multi-story seismic walls.
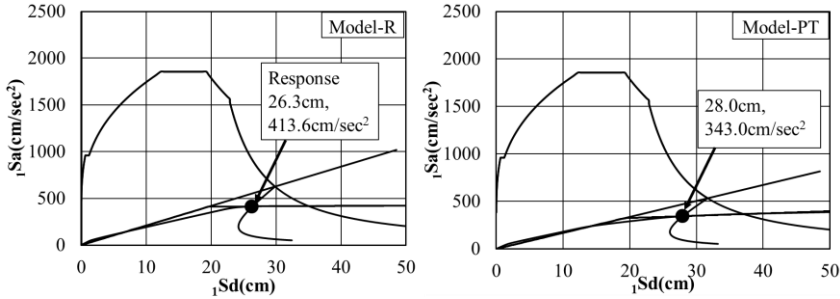
Figure 4. Response of the equivalent single-degree-of-freedom system according to the response spectrum method of Model-R and Model-PT in the X direction

5

Table 5. Response value and equivalent period of each model

X Direction				Y Direction			
Share Margin	$_1Sa$	$_1Sd$	T_e (s)	Share Margin	$_1Sa$	$_1Sd$	T_e (s)
1.0	337.9	28.0	1.535	1.0	517.2	24.3	1.178
1.1	343.0	28.0	1.532	1.1	519.1	24.3	1.176
1.2	349.3	28.0	1.523	1.2	520.3	24.2	1.169
1.3	355.7	27.9	1.518	1.3	520.5	24.0	1.162
1.4	359.7	27.8	1.509	1.4	520.7	24.0	1.159
1.5	364.9	27.7	1.502	1.5	521.6	23.9	1.157
Model-R	413.6	26.3	1.371	Model-R	522.5	23.5	1.131
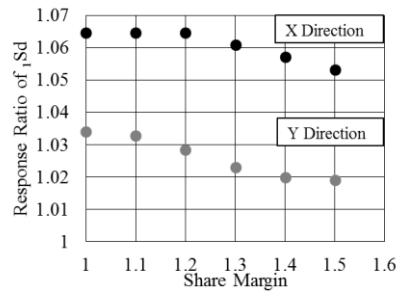
Figure 5. Relationship between the response ratio of $_1Sd$ and the joint shear margin

TIME HISTORY RESPONSE ANALYSIS

Maximum Story Shear Force and Maximum Story Drift Angle

Figure 6 and 7 show the distribution of maximum story shear force and the distribution of maximum story drift angle obtained by the time history response analysis, respectively. In the X direction, as the joint shear margin increases, the maximum story shear force increases and the maximum story drift angle decreases. On the other hand, in the Y direction, no significant difference was found about maximum story shear force and maximum story drift angle. The maximum story shear force of Model-R is greater than the maximum story shear force of Model-m15 in both the X and Y directions. The maximum story drift angle of Model-R is generally smaller than Model-m10. However, some exceptions due to seismic waves and the number of floors were found.
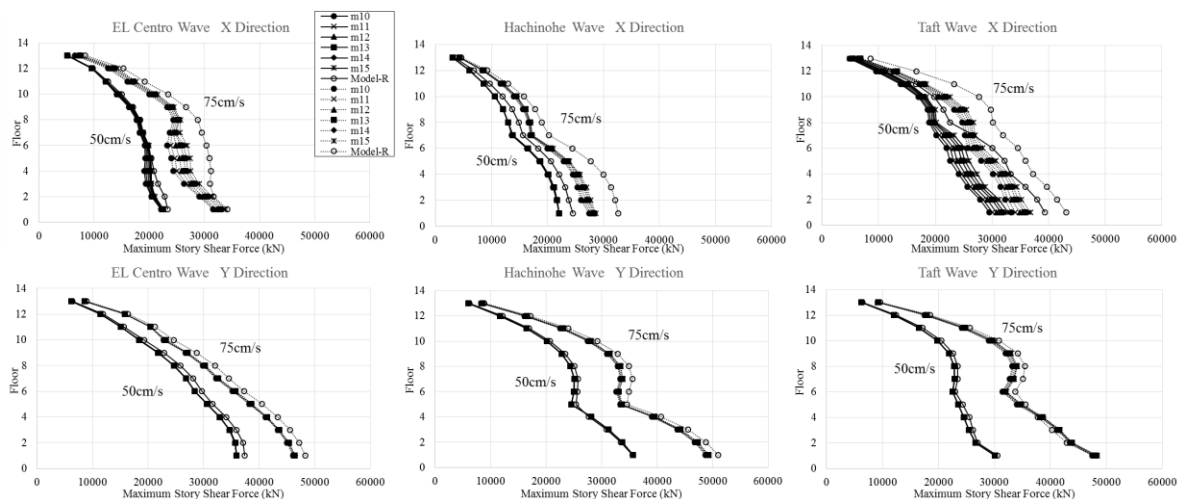
Figure 6. Distribution of maximum story shear force
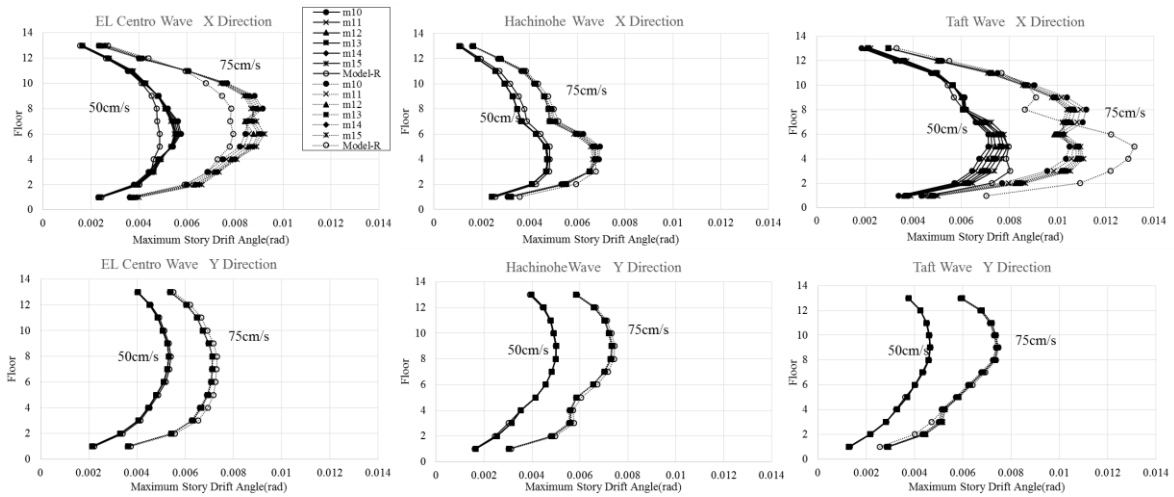
Figure 7. Distribution of maximum story drift angle

Relationship between Maximum Story Drift Angle and Beam-Column Joint Shear Margin

Figure 8 shows the relationship between the response ratio of the maximum story drift angle and the joint shear margin. The response ratio of the maximum story drift angle is obtained by dividing the maximum story drift angle of the panel zone model by the maximum story drift angle of Model-R. The response ratio in the X direction was 0.8 to 1.2. Therefore, the maximum story drift angle of the panel zone model showed an increase or decrease of about 20% as compared to the rigid zone model. The response ratio of the EL Centro wave 50 cm/s and the Hachinohe wave 75 cm/s decreased as the beam-column joint shear margin increased. The response ratio of the EL Centro wave 75 cm/s and the Taft wave 75 cm/s decreases until the beam-column joint shear margin of 1.2. However, the response ratio increases when the beam-column joint shear margin exceeds 1.2. In Hachinohe wave of 50 cm/s, the response ratio was hardly changed by the increase of the beam-column joint shear margin. The response ratio of the Taft wave 50 cm/s increased as the beam-column joint shear margin increased. Even if the joint shear margin increases, the response ratio does not decrease as Figure 5. In the Y direction, the response ratio was hardly changed by the difference of beam-column joint shear margin.
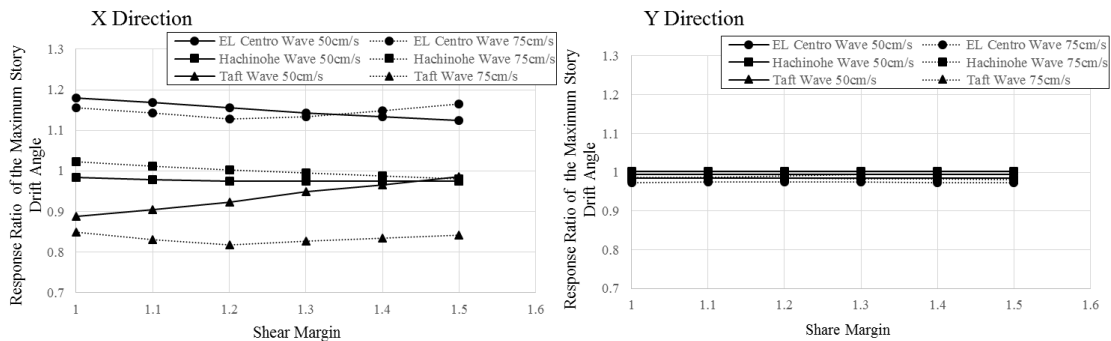
Figure 8. Relationship between the response ratio of the maximum story drift angle and the joint shear margin

Fluctuation Factor of Earthquake Response Value

In figure 3, the circle shows the horizontal displacement of 9th floor obtained from the time history response analysis as a representative displacement. The representative load of the X direction increases as the joint shear margin increases, but that of the Y direction slightly increases as the joint shear margin increases. Moreover, the difference of the representative load among the panel zone

models in the waves of 75 cm/s is more remarkable than that in the waves of 50 cm/s. Figure 9 shows the acceleration response spectra of EL Centro wave, Hachinohe wave and Taft wave. Figure 9 also shows the first natural period and the second natural period shown in Table 4. The response acceleration at the first natural period of Model-PT in EL Centro and Hachinohe waves is smaller than that of Model-R, but that of Model-PT in Taft wave is almost the same as that of Model-R. Therefore, it is thought that the story drift angle of Model-PT in Taft wave smaller than that of Model-R. The story drift angle of Model-R in the EL Centro wave is smaller than that of Model-PT because the response acceleration around the first natural period is relatively large compared with that of the Hachinohe wave. On the other hand, the Taft wave has a very large response acceleration around the second natural period compared with the EL Centro wave and the Hachinohe wave. As a results, the response of Taft wave is large because the second mode response appears more strongly.
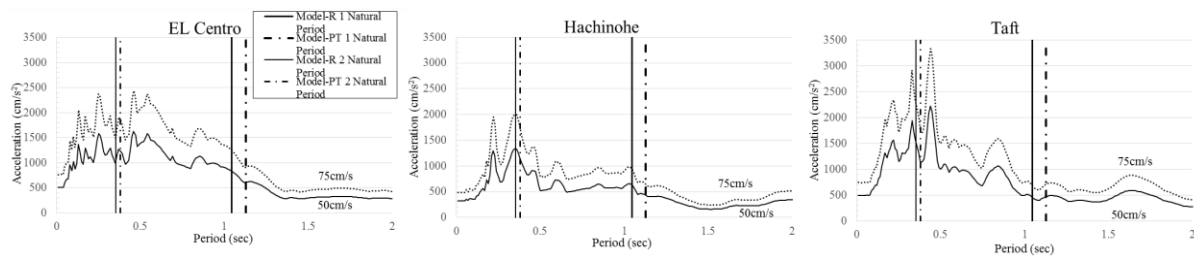
Figure 9. Acceleration response spectrum of EL Centro wave, Hachinohe wave and Taft wave

COMPARISON OF RESPONSE VALUES OF EQUIVALENT SINGLE-DEGREE-OF-FREEDOM SYSTEM AND TIME HISTORY RESPONSE ANALYSIS

Figure 10 shows the distribution of the response ratio of the story drift angle for each story in the EL Centro wave. The response ratio is obtained from dividing the maximum story drift angle of the panel zone model by the maximum story drift angle of Model-R for each story. Figure 11 shows the relationship between the response ratio of the maximum story drift angle and the joint shear margin derived by the time history response analysis. In this case, the response ratio was calculated for the response indicated by the circle in figure 10. Figure 11 shows the characteristics that the response ratio decreases as the joint shear margin increases, as with Figure 5. In the X direction, the response ratio of the equivalent single-degree-of-freedom system was at most 6.5% and the response ratio of the time history response analysis was up to 30%. The response of the panel zone model approaches the response of the rigid zone model as the shear margin increases in both analyses. In the Y direction, the response ration of the equivalent single-degree-of-freedom system was at most 3.5% and the response ratio of the time history response analysis was up to 14%. The response of the panel zone model was hardly fluctuated with the shear margin increase in both analyses except for the time history response of Taft wave of 75 cm/s.
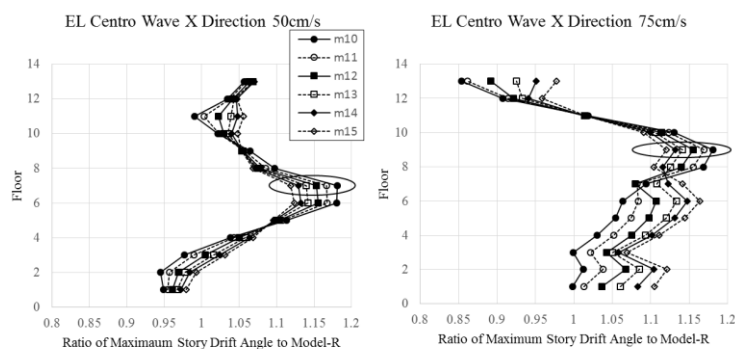
Figure 10. Distribution of the response ratio of the story drift angle for each story
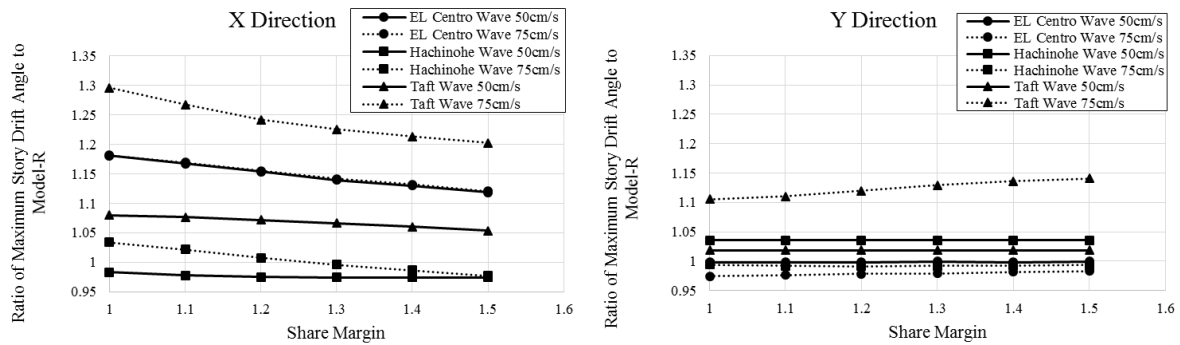
Figure 11. Relationship between the response ratio of the maximum story drift angle and the joint shear margin derived by the time history response analysis

CONCLUSIONS

MAP (Modal Adaptive Pushover) analysis and the time history response analysis were carried out for the model in which the shear strengths of beam-column joints were changed. Based on the results of MAP analysis, the response of the equivalent single-degree-of-freedom system was obtained. The earthquake response of the time history response analysis was obtained. The relationship between the response of CES building and the beam-column joint shear strength was clarified.

X Direction

・The response ratio of the equivalent single-degree-of-freedom system was at most 6.5%.
・The response of the panel zone model approaches the response of the rigid zone model as the shear margin increases in both analyses.

Y Direction

・The response of the equivalent single-degree-of-freedom system was at most 3.5%.
・The response of the panel zone model was hardly fluctuated with the shear margin increase in both analyses except for the time history response of Taft wave of 75 cm/s.

REFERENCES

Architectural Institute of Japan (2013).”Toward the establishment of guidelines for evaluation of structural performance of CES buildings,” *Annual Conference of Architectural Institute of Japan (Hokkaido), Division of Structural Engineering (SCCS) PD Material*, 1-67

Inoue, S., Akita. T and Inai. E (2015).” A Study on Applicability of CES Structural Performance Evaluation Method Using Trial Design Building, “*Architectural Institute of Japan Chugoku Chapter Research Report Collection*, 38, 249-252

Imai, T., Matukaze. Y, Suzkuki. T and Kuramoto. Y (2015).” A Study on Earthquake Response for CES Structural Building (Part 1 and 2),” *Academic Lecture Synopsis Collection of the Architectural Institute of Japan*, 1325-1328

Kuramoto, H. (2004),” Earthquake Response Characteristics of Equivalent SDOF System Reduced from Multi-Story Buildings and Prediction of Higher Mode Responses,” *Architectural Institute of Japan structure System Papers*, 580, 61-68,

Kuramoto, H., Teshigawara. M, Koshika. N and Isoda. H (2001).” Conversion of Multi-Story Building into Equivarent SDOF System and ITS Predictability Earthquake Response,” *Architectural Institute of Japan Structure System Papers*, 546, 79- 85,

Kuramoto, H. (2005),” CES Composite Structure System,” *Journal of Architectural and building sciense*, 120, 1535, 34-35,

Matsui, T. and Kuramoto. H (2011).” Effect of Applied Axial Forces on Structural Performance of CES Beam-Column Joints,” *Architectural Institute of Japan Structure System Papers*, 663, 1025-1031

Nakano, R., Akita. T and Inai. E (2016).” A Study on the Influence of the Beam Column Joint Model on the Seismic Performance of CES Structure,” *Architectural Institute of Japan Chugoku Chapter Research Report Collection*, 39, 213-216

Shi, J., Makimoto. R, J.J. Castro, Matui. T and Kuramoto. H (2012).” A Study on Evaluation of Deformation Capacity of CES Column with H-shaped Steel,” *Architectural Institute of Japan Structure System Papers*, 682, 1977-1982

Suzuki, S., Matui. T and Kuramoto. H (2011).” Non-Linear FEM Analysis for CES Shear Wall of Different Anchorage Condition of Longitudinal Wall Reinforcing Bars,” *Architectural Institute of Japan Structure System Papers*, 666, 1533-1540